Cryoturbation in the Central Brooks Range, Alaska

Nicolas A. Jelinski*

Winning Entry

2012 Graduate Student Paper Contest

Cryoturbation in permafrost-affected soils is important to many Arctic biogeochemical processes and critical to the appropriate classification of Gelisols. Standardized methodologies for describing the soils formed from these processes and knowledge regarding the time scales at which they operate continue to evolve. Twenty-six profiles were described across a transect in the Midas Lake region of the Central Brooks Range of Alaska using a modified version of the standard USDA and Turbel description protocol that is appropriate for work in wilderness areas. Profile descriptions and associated field data were aggregated and generalized to reveal major trends and relationships in horizonation between cryoturbated and noncryoturbated soils on the transect. A conceptual model for the geomorphic relationships of cryoturbated and noncryoturbated soils on this landscape was developed. In addition to a landscape-scale perspective, individual profiles were described on patterned ground features at a location where cryoturbated horizons were strongly expressed. Samples from these profiles were analyzed for cesium-137 (^{137}Cs) activity, and it was found that the surficial activity of this fallout radioisotope varied strongly by material type and position on the patterned ground microtopography. These differences suggest that the use of fallout isotopes, such as ^{137}Cs, when combined with quantitative profile descriptions and a standardized description protocol, may significantly improve our understanding of the spatial distribution and mechanisms of cryoturbation.

Cryoturbation plays a critical role in the formation of Arctic soils through ground patterning, the sequestration of organic matter below the soil surface, and alterations to the physical structure of soil materials (Bockheim and Hinkel, 2007; Kaiser et al., 2007; Ping, 2013). Additionally, the Turbel suborder and Turbic subgroups of other suborders are defined by the presence of cryoturbated horizons and gelic materials, which "are manifested by involuted, irregular, or broken horizons, organic matter near or within the permafrost table, oriented rock fragments, and silt enriched layers" (Bockheim et al., 1997; Soil Survey Staff, 2010). Thus the accurate mapping of Arctic soils and quantification of carbon in Arctic landscapes is dependent on our understanding of cryoturbation and related permafrost processes (Ping et al., 2013).

Large-scale latitudinal gradients and regional- to local-scale patterns of cryoturbation have been well characterized by U.S., Canadian, and Russian scientists (Zoltai and Tarnocai, 1981; Kokelj et al., 2007; Walker et al., 2008). Conceptual and quantitative models have been constructed that can adequately represent cryoturbation in some environments (Vandenberghe, 1992; Swanson et al., 1999; Peterson and Krantz, 2003; Nicolsky et al., 2008), but best practices for the description of these soils and knowledge regarding the rates at which these processes operate remain an evolving area of research (Bockheim, 2007; Ping et al., 2013). Cryoturbation can produce highly complex soil profiles, and therefore standardizing the description of these soils warrants supplemental procedures and methodologies (Ping et al., 2013). These methodologies require an inherent understanding of the multiscale variations in surficial patterns produced by cryoturbative processes as well as the landscape settings under which these processes should be expected to occur (Ping, 2013).

Additionally, quantifying the magnitude and timescales over which cryoturbation operates are critical to questions of Arctic soil genesis and predictions of future response to climate change (Bockheim, 2007). Although radiocarbon (^{14}C) and the fallout radioisotope lead-210 (^{210}Pb) have been used to constrain the age of individual buried organic horizons (Kaiser et al., 2007; Becher et al., 2013), radioisotope tools remain underutilized in studies of cryoturbation. Cesium-137 has long been used to infer the movement and mixing of soil materials at a landscape and profile scale (Ritchie and McHenry, 1990; Kaste et al., 2007). Both wet and dry ^{137}Cs deposition occurred following atmospheric testing of thermonuclear weapons in the 1950s and 1960s (Aoyama et al., 2006). Under most

Nicolas A. Jelinski, Ph.D. Candidate, Dep. of Soil, Water and Climate, Univ. of Minnesota-Twin Cities, 1991 Upper Buford Cir., St. Paul, MN 55108-6028. *Corresponding author (jeli0026@umn.edu).

doi:10.2136/sh13-01-0006
A peer-reviewed contribution published in *Soil Horizons* (2013).
Received 30 Jan. 2013.
Open access.

Abbreviations: AQP, Algorithms for Quantitative Pedology; MAAT, Mean Annual Air Temperature; MAST, Mean Annual Soil Temperature.

environmental conditions, this fallout ^{137}Cs adsorbs strongly to soil minerals and organic matter, and can be used to track soil movement over decadal timescales through spatial differences in measured activities (Matisoff and Whiting, 2011).

The objectives of this study were to utilize pedon descriptions across a transect in the Central Brooks Range of Alaska to demonstrate how this information can be used to produce a generalized view of the differences between cryoturbated and noncryoturbated soils and their relationships to landscape parameters. Additionally, I explore the qualitative use of ^{137}Cs as a potential tracer of soil movement due to cryoturbation across patterned ground and advocate for the future use of quantitative, spatially explicit sampling schemes that apply a suite of radioisotope tracers to further improve our knowledge of cryoturbation processes in Arctic soils.

Materials and Methods

Data and samples were collected in late July, 2012 as part of long-term monitoring work across the Arctic National Park network. The Midas Lake region of the Noatak River valley (67°48′ N, 156°15′ W) is located north of the Schwatka Mountains and approximately 40 km downstream of the headwaters of the Noatak River, in the western portion of Gates of the Arctic National Park, central Brooks Range, Alaska (Fig. 1). Although no direct temperature or precipitation observations are available for this area, modeling results predict mean annual air temperatures (MAAT) of −8°C and 450 to 500 mm of precipitation (PRISM Climate Group, 2012). Because mean annual soil temperatures (MAST) are typically 2°C higher than MAAT in Arctic and Subarctic regions (Smith et al., 1998), this site likely has an average MAST of approximately −6°C, which places the location within the gelic soil temperature regime. Modern alluvium and alluvial terrace deposits of Holocene age dominate the parent materials of the Noatak floodplain (elevation 500 m, 0–2% slopes), while glacial drift of Itkillik II Age (Late Pleistocene) and colluvium occupy the low moraines (2–5% slopes) and bedrock controlled foothills (10–20% slopes) of the surrounding mountains (Hamilton and Labay, 2011). At elevations to 1200 m, depth to schist bedrock is shallow (<20 cm), and most unconsolidated material is colluvial in nature.

Twenty-six soil profiles were described across a 4-km transect from the valley floor (500-m elevation) to an elevation of 700 m (Fig. 1). Vegetation ecotypes across the transect were characterized by Lowland Sedge-Dryas Meadow and Riverine Birch, Alder, and Low Willow Shrub tundra in the floodplain of the Noatak River; Upland Dwarf Birch-Tussock Shrub and Lowland Alder Tall Shrub tundra at mid elevations and south- and west-facing slopes; and Alpine Dryas Dwarf Shrub and Upland Birch-Ericaceous-Willow Low Shrub tundra at high elevations and north- and east-facing slopes (National Park Service, 2009).

Standard USDA description techniques (Soil Survey Staff, 2002) and the supplementary Turbel description protocol of Ping et al. (2013) were adapted to meet critical time, equipment, and sampling constraints in place due to work in a remote, National Park wilderness area. The organic and mineral components of gelic materials in cryoturbated horizons were described independently, with percentages of each material estimated over the entire horizon interval. Pit excavation was limited to the depth of hand tool refusal by frozen or lithic material or maximum depth of the implement (typically 40–140 cm) because power tools were not permitted in the wilderness area. Excavated pit size was limited to 40 by 40 cm to accommodate archeological considerations. Evidence of irregular or broken boundaries, the presence of gelic materials, and surficial microtopography were used to identify cryoturbated horizons in instances where pit dimensions prohibited the observation of involutions. A pH testing kit (La Motte Model ST-M) was used to record approximate pHs of individual horizon components

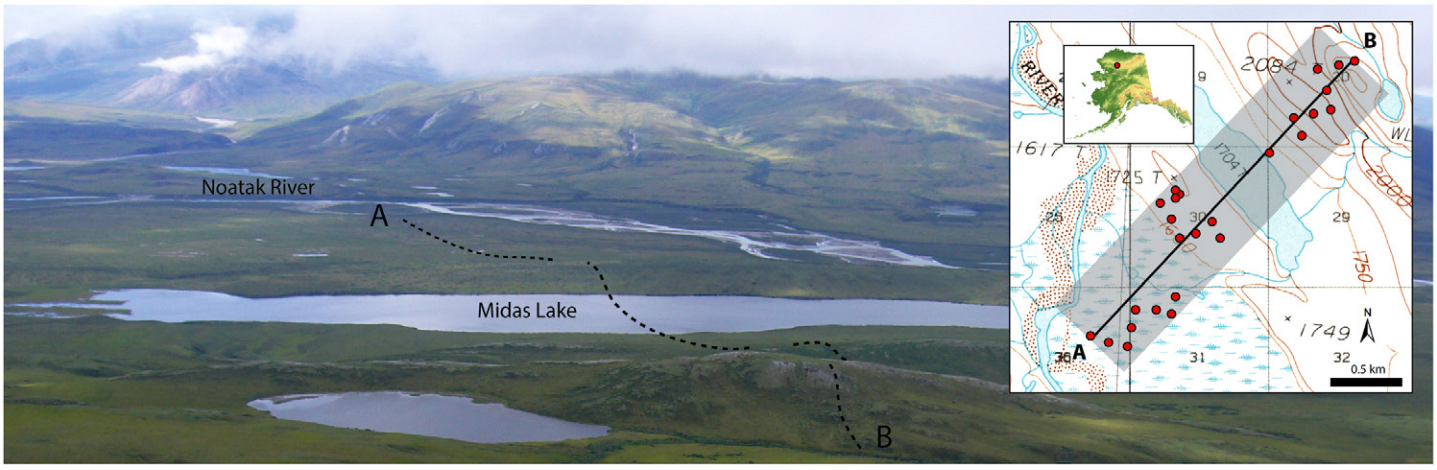

Fig. 1. Geographic location and landscape setting of Midas Lake transect, Brooks Range, Alaska. Soil profiles were described across the transect within the gray bar. Inset topographic map: USGS Ambler River Quadrangle, 1990 (elevations in feet).

on soil slurries in the field. To demonstrate broad soil–landscape relationships, soils were classified into subgroups from field descriptions (Soil Survey Staff, 2010) and generalized across the transect. The R-based package Algorithms for Quantitative Pedology (AQP) (Beaudette et al., 2013) was used to visualize horizon information and properties from field descriptions as well as to conduct data aggregation and generalization. Statistical analyses were conducted using native algorithms in R 3.0 (R Development Core Team, 2011).

Restrictions on pit size did not allow the sampling of full cycles of patterned ground as recommended by Ping et al. (2013), so three individual profiles were excavated across a single cycle at one location with strong patterned ground expression (Fig. 2, location 2) to provide a complete "snapshot" of variability. Five to six samples were taken from each profile at average depths of 5, 10, 20, 30, and 40 cm (Fig. 3). These samples were sieved to remove coarse fragments and roots >2 mm, and analyzed for ^{137}Cs activity by gamma spectrometry. Samples for gamma spectrometry were packed into glass vials and counted for 24 h on a high-purity Germanium crystal well detector (Canberra, Inc.). Final activities and uncertainties were calculated by applying energy and efficiency calibrations to the gamma spectrum with reference to the ^{137}Cs characteristic 661.6-keV peak. Uncertainties in ^{137}Cs activities were generally around 10% of measured values.

Although the Fukushima Daiichi nuclear incident occurred before the sampling of these soils, the estimated deposition of ^{137}Cs due to the Fukushima incident in this region of the Brooks Range is 10 to 100 Bq m^{-2} (Christoudias and Lelieveld, 2012; Stohl et al., 2011). This is still about an order of magnitude lower than the ^{137}Cs activity expected to remain on the land surface in the Central Brooks Range from atmospheric weapons testing in the mid 1960s (3000–4000 Bq m^{-2} by January 1970 [Aoyama et al., 2006] and 1100–1900 Bq m^{-2} at time of sampling in late July 2012), so this deposition of ^{137}Cs has likely had minimal impact on these results. Furthermore, it is likely that ^{137}Cs fallout from Fukushima Daiichi would be uniformly distributed across landscape elements, potentially influencing total activity but not changing the qualitative interpretation of the relative activities of surficial materials.

Results

General Soil Characteristics and Horizonation

Generalizing profile descriptions and field pH measurements by groups based on the presence of cryoturbated soil horizons and landscape positions revealed important trends in the data (Fig. 4). The average depth of observation for noncryoturbated soils along the transect was 44 cm. Observation depth was restricted by consolidated (noncryoturbated upland soils) or frozen materials (noncryoturbated lowland soils) (Fig. 4B and 4C). All noncryoturbated profiles had organic materials at the surface (Fig. 4B and 4C). Noncryoturbated profiles in lowland landscape positions were characterized by the thickest surficial organic layers (an average of 26 cm), while noncryoturbated soils on uplands had an average depth of organic layer to 9 cm and shallow depth to schist bedrock (33 cm).

In contrast, many of all cryoturbated profiles did not have a continuous organic layer at the surface. Instead, cryoturbated

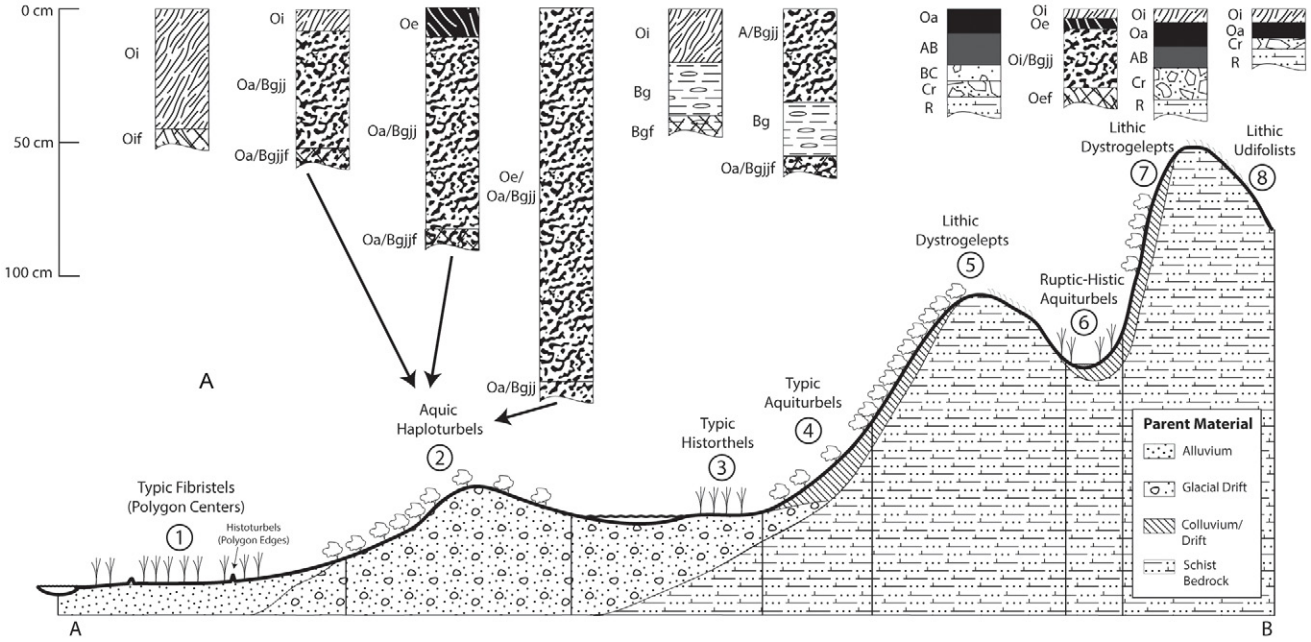

Fig. 2. Generalized soil–landscape relationships across Midas Lake transect. Points A and B at bottom of bar refer to the same points in Fig. 1. Vertical elevations are exaggerated.

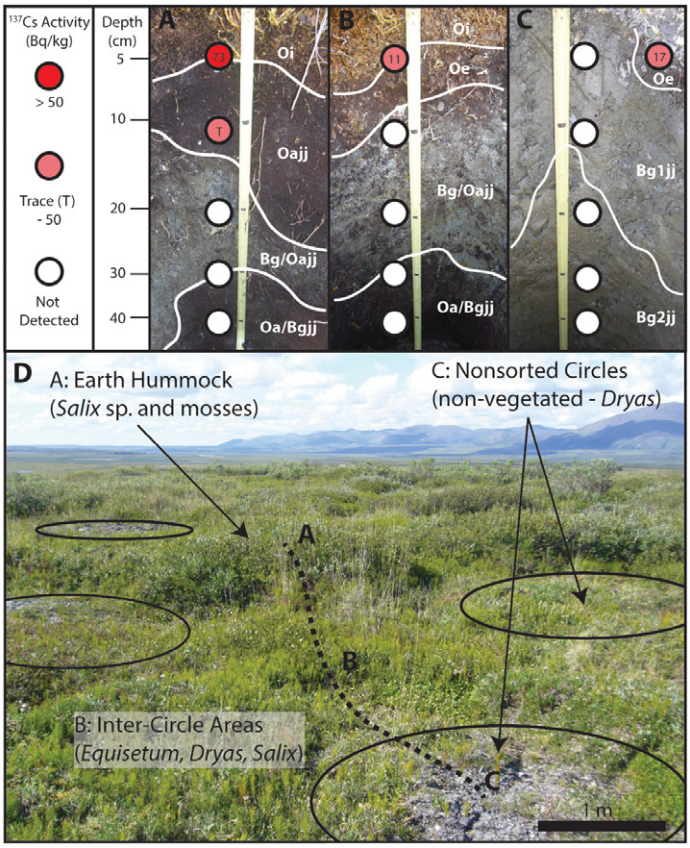

Fig. 3. Overview of patterned ground microtopography, cryoturbated soil profiles and observed activities of ^{137}Cs at transect location 2 (moraine). Letters above soil profile pictures refer to letters of surficial features in overview photograph. Numbers inside shaded circles denoting ^{137}Cs activity range indicate measured values.

horizons containing gleyed subsoil were exposed at the surface in almost one-half of all observed profiles (Fig. 4A). Horizon generalization across cryoturbated profile descriptions revealed a peak probability of cryoturbated horizon identification ~30 cm, consistent with evidence of organic material being subducted below the surface, near the top of the permafrost table (Nicolsky et al., 2008). For those cryoturbated soils that had frozen layers encountered in excavation, the frozen layer was present at an average of 47 cm and represents a reasonable assumption of permafrost depth in these soils given that they were sampled in late July. Importantly, five of the sixteen cryoturbated profiles were unfrozen to a depth of at least 140 cm (maximum depth of implement penetration).

The presence of subsoil material and patchy or broken organic horizons at the surface in many of the cryoturbated soils was reflected in the observed field pH differences between cryoturbated (n = 16) and non cryoturbated (n = 10) profiles (Fig. 4D). These differences were highly significant both when pH observations were aggregated throughout the entire profile depth (6.85 and 6.01, $p < 0.001$ for cryoturbated and noncryoturbated soils, respectively, according to Welch's two sample T-Test) and when only the top 44 cm (the average depth of observation for noncryoturbated profiles) was considered (6.69 and 6.01, $p < 0.001$ for cryoturbated and noncryoturbated soils, respectively, according to Welch's two sample T-Test).

Soil–Landscape Relationships

Across the lowest portions of the landscape, on the floodplain of the Noatak River (Fig. 2, location 1), weakly expressed low-center polygons dominated the ground pattern. Extended periods of saturation have led to the development of Typic

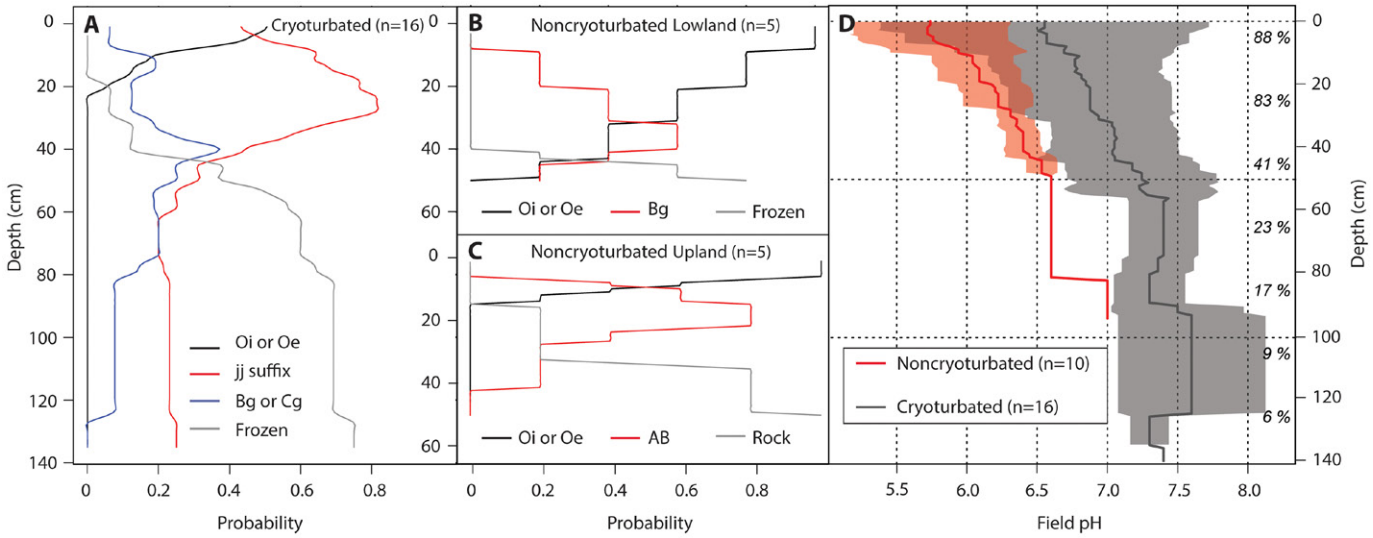

Fig. 4. Aggregated and generalized horizonation for soils across Midas Lake transect. Horizon probability distributions with depth as a fraction of total profiles for (A) cryoturbated soils, (B) noncryoturbated lowland soils, and (C) noncryoturbated upland soils. Frozen and rock layers noted in the field were assumed to extend with depth for visualization purposes only. (D) Field pH values with depth for cryoturbated and noncryoturbated soils; group means are represented by the solid lines, shaded range represents 25th and 75th percentiles. Percentages on the right are percent of total profiles contributing values with depth. All analyses conducted in AQP (Beaudette et al., 2013).

Fibristels, with thick organic mats composed of fibric materials that provide efficient insulation for the underlying frozen layer, further promoting episaturation due to strong limitations on infiltration. Because only the surficial organic materials in these soils thaw during the growing season, they are relatively static under current climate regimes. The exception to this was on the high polygon boundaries (making up <1% of this portion of the landscape), where the combination of surface heave due to the presence of ice wedges and elevation above the water table produced cryoturbated organic materials (Ping et al., 2013). Although no formal description was completed on these polygon boundaries, informal observations matched those described in similar conditions by Ping et al. (2013).

Across the low moraine composed of glacial drift (Fig. 2, location 2), soils were high enough above the water table to permit aquic conditions without permanent saturation, and the ground pattern was dominated by nonsorted circles, one of the most typical surficial patterns indicative of cryoturbative processes (Nicolsky et al., 2008). These non-sorted circles were only slightly vegetated (<20% cover) and profiles were well mixed. In addition to non-sorted circles on this landform, inter-circle areas and earth hummocks were part of the full cycle of patterned ground (Fig. 3D). Because non-sorted circles were highly expressed at this location, profiles representative of all patterned ground features were described (Fig. 2 and 3). The profile descriptions below illustrate some of the variability between individual profiles on separate microforms at this location (Fig. 3A and 3C):

Moraine Profile A (Fig. 3A)

Oi: 0–8 cm (14% of profile to 53 cm depth): black (7.5YR 2/1) and brown (7.5YR 4/4) peat; many very fine, fine and common medium roots; abrupt boundary.

Oajj: 7–32 cm (28% of profile to 53 cm depth): black (7.5YR 2/1) muck, common very fine, fine and medium roots; abrupt broken boundary.

Bg/Oajj: 7–42 cm: (33% of profile to 53 cm depth): grey (5Y 5/1) and greyish olive (5Y 4/2) gravelly fine sandy loam; 20% brownish black (10YR 3/2) medium blocks of highly decomposed muck; weak fine to moderate subangular blocky structure and weak thin platy structure; friable; nonsticky and nonplastic; few very fine to fine roots; abrupt broken boundary.

Oa/Bgjj: 30–42 cm (22% of profile to 53 cm depth): black (7.5YR 2/1) muck; 15% grey (5Y 5/1) coarse blocks of firm very gravelly fine sandy loam; common very fine, fine and medium roots; abrupt broken boundary.

Oaf: 42–44 cm (3% of profile to 53 cm depth): black (7.5YR 2/1) muck; extremely firm.

Moraine Profile C (Fig. 3C)

Oejj: 0–12 cm (1% of profile to 140 cm depth): black (7.5YR 2.5/1) mucky peat; many very fine, fine, and few medium roots; abrupt broken boundary.

Oajj: 8–54 cm (3% of profile to 140 cm depth): black (7.5YR 2/1) muck; common very fine, fine, and medium roots; abrupt broken boundary.

Bg1jj: 0–82 cm (37% of profile to 140 cm depth): gray (5Y 4/1) and grayish olive (5Y 4/2) very gravelly fine sandy loam; moderate fine to coarse subangular blocky structure and moderate thin platy structure; friable; nonsticky and nonplastic; few very fine and medium roots; clear broken boundary.

Bg2jj: 12–95 cm (28% of profile to 140 cm depth): gray (5Y 5/1) very gravelly fine sandy loam; Fe concentrations (2.5Y 4/4) as distinct coarse masses; moderate medium subangular blocky structure and weak thin platy structure; friable, nonsticky and nonplastic; clear broken boundary.

Bg3jj: 52–140 cm (31% of profile to 140 cm depth): grayish olive (5Y 4/2) very gravelly fine sandy loam; 10% brownish black (10YR 3/2) coarse blocks of highly decomposed muck; moderate fine to coarse medium subangular blocky structure; friable; nonsticky and nonplastic.

To the east of Midas Lake, a low-relief plain underlain by glacial drift with highly saturated soils was dominated by *Carex* spp. tussocks (Fig. 2, location 3). Much like the Noatak River floodplain with thick, insulating organic materials at the surface, cryoturbated horizons were not observed at this location. Instead, soils were classified as Typic Historthels, with a thick, saturated mat of fibric material over mineral soil. Only on the upper toeslopes and lower backslopes of the adjacent, drift mantled hill (Fig. 2, location 4) were drainage conditions appropriate for cryoturbation to be manifested in soil profiles. Here, again, ground pattern was dominated by nonsorted circles. Although strong evidence of cryoturbation was apparent, soils also showed evidence of colluvial influence due to hillslope position. This was apparent from the presence of an A/Bgjj surficial horizon, which contained much more homogeneous and mixed organic material than the O/Bgjj horizons on the moraine.

Above these landscape positions, with increasing slopes, colluvial processes (i.e., solifluction lobes and colluvial deposits) overwhelmed any signal from cryoturbation; therefore, on the upper backslope, shoulder, and summit positions (Fig. 2, location 5), soils were shallow and poorly developed Lithic Dystrogelepts. The classification of these soils as Inceptisols in a gelic soil temperature regime may seem surprising, but the classification is based on the best available evidence from the field and is not an uncommon phenomenon (Ping, 2013). First, these soils are shallow to schist bedrock and have relatively thin insulating organic layers. This means that the thawing front likely advances at least a meter into the bedrock on most years, as has been observed in other sites at similar latitudes (Smith et al., 2010). Further, some cryoturbated soils just 100 to 150 m in elevation below these soils were not frozen to depths of at least 140 cm, suggesting that if the thawing front penetrated deeply into unconsolidated materials at this site, it could penetrate at least as deep into consolidated materials due to higher thermal conductivities (Guglielmin et al., 2011).

At the small basin saddle position (Fig. 2, location 6) weak nonsorted circle patterns were observed and were indicative of the underlying cryoturbated soils, which were classified as Ruptic-Histic Aquiturbels. At the highest elevations (Fig. 2, locations 7 and 8), Lithic Dystrogelepts dominated where depths to underlying consolidated materials were deeper than 20 cm and Lithic Udifolists where depths to bedrock were very shallow and organic materials overlie weathered bedrock. Paralithic materials were present as partially weathered (frost-shattered) and weakly cemented schist—these materials are described as Cr horizons at transect locations 5, 7, and 8 (Fig. 2). As elevation increased beyond point B, little to no unconsolidated materials were present and exposed, frost-shattered bedrock and tors dominated the landscape.

Quantifying Patterned Ground Movement Using Cesium-137 as a Tracer

The results of the small-scale sampling at location 2 (Fig. 3) along the transect showed that surficial ^{137}Cs activities can be highly heterogeneous across very short spatial scales on patterned ground features (Fig. 3A–3C). Most strikingly, samples collected from nonvegetated Bgjj material at the surface and small, isolated patches of Oe material in the circle center show significant differences in activities (Fig. 3C). While no ^{137}Cs could be detected in the Bgjj material, 17 Bq kg^{-1} was detected in the adjacent Oe. It is not surprising that no ^{137}Cs was detected in subsurface horizons because the profiles were sampled in the center and edge of the nonsorted circle to characterize maximum variability. The most recently subducted material would be expected to lie somewhere just in from the circle edge, which would only be captured with extensive grid sampling. Nevertheless, these results demonstrate the potential of ^{137}Cs to track the movement of soil materials at small scales on cryoturbated landforms.

Ceisum-137 was not detected below 15 cm in these samples, so it is likely that these soils adsorb and retain most of the ^{137}Cs fallout inventory without leaching to underlying horizons. Material with measurable ^{137}Cs was therefore likely present at or near the soil surface when the majority of atmospheric fallout occurred between 1958 and 1971 (Aoyama et al., 2006) while the absence of ^{137}Cs indicates the material was buried around the same time period and subsequently exhumed. This independently confirms the upward movement of subsoil materials in the nonsorted circle center on at least decadal timescales, and should be expected as these nonsorted circles remain largely vegetation free (or at least sparsely vegetated, even at lower latitudes sites such as this study area). Additionally, the lower activities in the inter-circle areas relative to the organic rich earth hummock (Fig. 3A–3C) could suggest that there has been a mechanism of loss of ^{137}Cs from the surface of the intercircle areas. One potential mechanism for this reduced activity is the subduction of surficial organic matter below the surface on time scales of 40 yr or less.

Alternative explanations for the lack of ^{137}Cs activity in the surficial Bgjj material at the circle center may include the differential deposition of ^{137}Cs across microtopography or small-scale wind erosion from the exposed circle center. Additionally, the mineral soil may have lower infiltration rates compared to surrounding organic materials when accumulated snow is melting in the spring and early summer. This may lead to runoff away from the higher elevation circle centers. If any of these were true, however, we would expect the highest ^{137}Cs activities in the low elevation intercircle areas. Instead, the highest activities were present in the organic materials of the earth hummock, the highest elevation microtopographic element of the ground pattern (Fig. 3D).

Discussion and Conclusions

This work shows that in remote areas with significant sampling constraints, modifications of existing protocols can still produce relevant information that can be utilized to characterize cryoturbated and noncryoturbated soils at the profile and landscape scales. The aggregation of field data through the use of quantitative analysis such as the algorithms provided in the AQP package (Beaudette et al., 2013) holds significant promise for generalizing profile descriptions from highly complex cryoturbated soils. Analysis of field pH measurements demonstrated that cryoturbation not only influences profile physical properties and horizonation, but also master environmental variables such as pH through the movement of surficial materials.

The identification of areas dominated by cryoturbated soils from surficial characteristics and the quantitative description of these soils through standardized methodologies is critical for advancing our knowledge of the distribution and global importance of these soils (Ping et al., 2013). Through this case study and the use of a modified version of a new standardized Turbel description protocol (Ping et al., 2013), the descriptions show that cryoturbated soils can be expected to occur in distinct positions on high-relief landscapes, where moisture regime is appropriate, unconsolidated materials are available, and disturbance from other processes such as colluvial transport do not overwhelm any signal from cryoturbation. This is in agreement with a qualitative soil description and classification previously undertaken by the National Park Service in Arctic Parklands (National Park Service, 2009) and with research on the spatial distribution of cryoturbated soils in other regions (Luoto and Hjort, 2004; Feuillet, 2011).

The application of ^{137}Cs and other radionuclides to track soil movement in landscapes such as this is a promising approach to quantify processes that have occurred during the past 50 years. Understanding the rates at which cryoturbative processes operate is critical for understanding how these soils will respond to future changes in climate. The results presented show that naturally occurring fallout radionuclides (in this case ^{137}Cs) have the potential to constrain rates and processes of movement in cryoturbated soils. Further work that characterizes a suite of radionuclides (i.e., ^{137}Cs,

^{210}Pb, and ^{14}C) using a horizontally and vertically gridded sampling scheme across multiple cycles of patterned ground would provide an opportunity to demonstrate the power of this approach.

Significant progress has now been made in standardizing these descriptions and linking them explicitly to sampling protocols. It is anticipated that future investigations will be able to utilize these approaches to improve on and advance our knowledge of how cryoturbation is distributed across diverse Arctic landscapes as well as how it functions to produce these dynamic and unique soils.

Acknowledgments

My special thanks to Dr. Dave Swanson of the National Park Service's Arctic Research Coordination Network for guidance and interpretations provided in the conception and review of this manuscript and to Fleur Nicklen and Marta Roser for their assistance in the field and laboratory. Many thanks to Dr. Kyungsoo Yoo for providing gamma spectrometer time and to Dr. Ed Nater, Dr. Brent Dalzell, and Dr. Terry Cooper of the University of Minnesota Department of Soil, Water, and Climate for their critiques on initial drafts. Lastly, I thank two anonymous reviewers for providing critical perspectives that have significantly improved this manuscript. This work was supported in part by NSF Graduate Research Fellowship 2011122508 to N.A. Jelinski.

References

Aoyama, M., K. Hirose, and Y. Igarashi. 2006. Re-construction and updating our understanding on the global weapons tests ^{137}Cs fallout. J. Environ. Monit. 8:431–438. doi:10.1039/b512601k

Beaudette, D.E., P. Roudier, and A.T. O'Geen. 2013. Algorithms for quantitative pedology: A toolkit for soil scientists. Comput. Geosci. 52:258–268. doi:10.1016/j.cageo.2012.10.020

Becher, M., C. Olid, and J. Klaminder. 2013. Buried soil organic inclusions in non-sorted circles fields in northern Sweden: Age and Paleoclimatic context. J. Geophys. Res. Biogeosci. 118:104–111. doi:10.1002/jgrg.20016

Bockheim, J.G., C. Tarnocai, J.M. Kimble, and C.A.S. Smith. 1997. The concept of gelic materials in the new gelisol order for permafrost-affected soils. Soil Sci. 162:927–939. doi:10.1097/00010694-199712000-00008

Bockheim, J.G. 2007. Importance of cryoturbation in redistributing organic carbon in permafrost-affected soils. Soil Sci. Soc. Am. J. 71:1335–1342. doi:10.2136/sssaj2006.0414N

Bockheim, J.G., and K.M. Hinkel. 2007. The importance of "deep" organic carbon in permafrost-affected soil of Arctic Alaska. Soil Sci. Soc. Am. J. 71:1889–1892. doi:10.2136/sssaj2007.0070N

Christoudias, T., and J. Lelieveld. 2012. Modelling the global atmospheric transport and deposition of radionuclides from the Fukushima Dai-ichi nuclear accident. Atmos. Chem. Phys. Discuss. 12:24531–24555. doi:10.5194/acpd-12-24531-2012

Feuillet, T. 2011. Statistical analyses of active patterned ground occurrence in the Taillon Massif (Pyrenees, France/Spain). Permafrost Periglac. Processes 22:228–238.

Guglielmin, M., M.R. Balks, L.S. Adlam, and F. Baio. 2011. Permafrost thermal regime from two 30-m deep boreholes in southern Victoria Land, Antarctica. Permafrost Periglac. Processes 22:129–139. doi:10.1002/ppp.715

Hamilton, T.D., and K.A. Labay. 2011. Surficial geologic map of the Gates of the Arctic National Park and Preserve, Alaska. USGS Scientific Investigations Map 3125, scale 1:300,000. http://pubs.usgs.gov/sim/3125/ (accessed 12 Aug. 2013).

Kaiser, C., H. Meyer, C. Biasi, O. Rusalimova, P. Barsukov, and A. Richter. 2007. Conservation of soil organic matter through cryoturbation in arctic soils in Siberia. J. Geophys. Res. 112:G02017. doi:10.1029/2006JG000258

Kaste, J.M., A.M. Heimsath, and B.C. Bostick. 2007. Short-term mixing quantified with fallout radionuclides. Geology 35:243–246. doi:10.1130/G23355A.1

Kokelj, S.V., C.R. Burn, and C. Tarnocai. 2007. The structure and dynamics of earth hummocks in the subarctic forest near Inuvik, Northwest Territories, Canada. Arct. Antarct. Alp. Res. 39:99–109. doi:10.1657/1523-0430(2007)39[99:TSADOE]2.0.CO;2

Luoto, M., and J. Hjort. 2004. Generalized linear modeling in periglacial studies: Terrain parameters and patterned ground. Permafrost Periglac. Processes 15:327–338. doi:10.1002/ppp.482

Matisoff, G., and P.J. Whiting. 2011. Measuring soil erosion rates using natural (^{7}Be, ^{210}Pb) and anthropogenic (^{137}Cs, ^{239,240}Pu) radionuclides. In: M. Baskaran, editor, Handbook of environmental isotope geochemistry. Advances in Isotope Geochemistry. Springer-Verlag, Berlin, Heidelberg. p. 487–488

National Park Service. 2009. An ecological land survey and landcover map of the Arctic network. Natural Resource Technical Report NPS/ARCN/NRTR-2009/270.

Nicolsky, D.J., V.E. Romanovsky, G.S. Tipenko, and D.A. Walker. 2008. Modeling biogeophysical interactions in non-sorted circles in the low Arctic. J. Geophys. Res. 113:G03S05. doi:10.1029/2007JG000565

Peterson, R.A., and W.V. Krantz. 2003. A mechanism for differential frost heave and its implications for patterned-ground formation. J. Glaciol. 49:69–80. doi:10.3189/172756503781830854

Ping, C.-L. 2013. Gelisols: Part I. Cryogenesis and state factors of formation. Soil Horiz. 54(3). doi:10.2136/sh2013-54-3-gc

Ping, C.-L., M.H. Clark, J.M. Kimble, G.J. Michaelson, Y. Shur, and C.A. Stiles. 2013. Sampling protocols for permafrost-affected soils. Soil Horiz. 54(1). doi:10.2136/sh12-09-0027

PRISM Climate Group. 2012. PRISM Climate Group, Oregon State University. http://prism.oregonstate.edu (accessed 12 Aug. 2013).

R Development Core Team. 2011. R: A language and environment for statistical computing. R Foundation for Statistical Computing, Vienna, Austria.

Ritchie, J.C., and J.R. McHenry. 1990. Application of radioactive fallout Cesium-137 for measuring soil erosion and sediment accumulation rates and patterns: A review. J. Environ. Qual. 19:215–233. doi:10.2134/jeq1990.00472425001900020006x

Smith, C.A.S., C.R. Burn, C. Tarnocai, and B. Sproule. 1998. Air and soil temperature relations along an ecological transect through the permafrost zones of northern Canada. In: Proceedings of the Seventh International Conference on Permaforst, Yellowknife, Canada. International Permafrost Association, Potsdam, Germany. p. 1009–1015.

Smith, S.L., V.E. Romanovsky, A.G. Lewkowicz, C.R. Burn, M. Allard, G.D. Clow, K. Yoshikawa, and J. Throop. 2010. Thermal state of permafrost in North America: A contribution to the International Polar Year. Permafrost Periglac. Processes 21:117–135. doi:10.1002/ppp.690

Soil Survey Staff. 2002. Field book for describing and sampling soils. Version 2.0. NRCS-NSSC, Lincoln, NE.

Soil Survey Staff. 2010. Keys to soil taxonomy. 11th ed. USDA-NRCS, Washington, DC.

Swanson, D.K., C.L. Ping, and G.J. Michaelson. 1999. Diapirism in soils due to thaw of ice-rich material near the permafrost table. Permafrost Periglac. Processes 10:349–367. doi:10.1002/(SICI)1099-1530(199910/12)10:4<349::AID-PPP318>3.0.CO;2-N

Stohl, A., P. Siebert, G. Wotawa, D. Arnold, J.F. Burkhart, S. Eckhardt, C. Tapia, A. Vargas, and T.J. Yasunari. 2011. Xenon-133 and caesium-137 releases into the atmosphere from the Fukushima Dai-ichi nuclear power plant: Determination of the source term, atmospheric dispersion, and deposition. Atmos. Chem. Phys. Discuss. 11:28319–28394. doi:10.5194/acpd-11-28319-2011

Vandenberghe, J. 1992. Cryoturbations: A sediment structural analysis. Permafrost Periglac. Processes 3:343–352. doi:10.1002/ppp.3430030408

Walker, D.A., H.E. Epstein, V.E. Romanovsky, C.-L. Ping, G.J. Michaelson, R.P. Daanen, Y. Shur, R.A. Peterson, W.B. Krantz, M.K. Raynolds, W.A. Gould, G. Gonzalez, D.J. Nicolsky, C.M. Vonlanthen, A.H. Kade, P. Kuss, A.M. Kelley, C.A. Munger, C.T. Tarnocai, N.V. Matveyeva, and F.J.A. Daniels. 2008. Arctic patterned-ground ecosystems: A synthesis of field studies and models along a North American Arctic Transect. J. Geophys. Res. 113:G03S01. doi:10.1029/2007JG000504

Zoltai, S.C., and C. Tarnocai. 1981. Some nonsorted patterned ground types in northern Canada. Arct. Alp. Res. 13:139–151. doi:10.2307/1551191